

the Θ^{-1} distribution of Fig. 2 peaks near this value. For $\eta \rightarrow \pi^0 + \gamma + \gamma$ events, the phase-space spectrum of $M_{\gamma\gamma}$ produces a corresponding spread of θ_2 values, thus smearing out the Θ^{-1} distribution as shown in Fig. 2.

Clearly, any model of the decay $\eta \rightarrow \pi^0 + \gamma + \gamma$ which seriously distorts the $M_{\gamma\gamma}$ phase-space spectrum will affect our upper limit for r . One particular model of η decay has been considered.⁵ Taking the η as an initial quark-antiquark state, it is assumed to decay via two successive magnetic dipole transitions: $\eta \rightarrow \rho^0 + \gamma$, $\rho^0 \rightarrow \pi^0 + \gamma$, where the ρ^0 represents a virtual 1^- intermediate state (the ρ^0 , ω^0 , or ϕ^0). This model produces a flattening of the $M_{\gamma\gamma}$ spectrum compared to pure phase space, but leaves unchanged the upper limit for r .

(d) It has been determined³ that there is a background of 15 to 40% in the low-mass region of the 4γ data [threshold to 1.0 BeV in Fig. 1(b)], due to feed-down from $3\pi^0$ events in which two of the six gammas have escaped detection. We have not been able to predict all the detailed properties of such feed-down events, but reasonable models predict Θ^{-1} distributions which are broader than the observed experimental Θ^{-1} distribution. Therefore, introduction of these background events into the fits to the 4γ data will decrease the number of $\eta \rightarrow \pi^0 + \gamma + \gamma$ events in the best fit; in fact, a reasonable fit can be obtained using only $\pi^0\pi^0$ events plus $3\pi^0$

feed-down events, with no η 's. For this reason, the value of r determined above, which assumed the existence of only $\pi^0\pi^0$ and $\eta \rightarrow \pi^0 + \gamma + \gamma$ events in the data, is considered an upper limit rather than an exact determination.

We wish to thank Professor B. T. Feld for his calculations and discussions of η decay, and Professor D. H. Frisch, Dr. P. M. Mockett, and Dr. A. H. Rogers for several helpful discussions.

*This work is supported in part through funds provided by the U. S. Atomic Energy Commission under Contract No. AT(30-1-2098). This research was performed using the Alternating Gradient Synchrotron at Brookhaven National Laboratory.

¹G. Di Giugno, R. Querzoli, G. Troise, F. Vanoli, M. Giorgi, P. Schiavon, and V. Silvestrini, Phys. Rev. Letters **16**, 767 (1966).

²L. Sodickson, M. Wahlig, I. Mannelli, D. Frisch, and O. Fackler, Phys. Rev. Letters **12**, 485 (1964); M. A. Wahlig *et al.*, Phys. Rev. Letters **13**, 103 (1964); M. A. Wahlig *et al.*, in Proceedings of the Twelfth International Conference on High Energy Physics, Dubna, 1964 (Atomizdat., Moscow, 1966); I. Mannelli, A. Bigi, R. Carrara, M. Wahlig, and L. Sodickson, Phys. Rev. Letters **14**, 408 (1965).

³M. Wahlig, E. Shibata, D. Gordon, D. Frisch, and I. Mannelli, to be published.

⁴O. Guisan, J. Kirz, P. Sonderegger, A. V. Stirling, P. Borgeaud, C. Bruneton, P. Falk-Vairant, B. Amblard, C. Caversasio, J. P. Guillaud, and M. Yvert, Phys. Letters **18**, 200 (1965).

⁵B. T. Feld, private communication.

MEASUREMENT OF THE Σ^+ MAGNETIC MOMENT*

V. Cook, T. Ewart,† G. Masek,‡ R. Orr,§ and E. Platner||
Physics Department, University of Washington, Seattle, Washington
(Received 2 February 1966)

This paper presents the results of a measurement of the magnetic moment of the Σ^+ hyperon. In addition to providing a test of current baryon symmetry schemes, the experiment also demonstrates the feasibility of several new techniques in experimental high-energy physics. Spark chambers were operated directly in very high (165 kG) magnetic fields, and spark-chamber observations were made of the complete production and decay event of the short-lived sigma hyperon (see Fig. 1). The general method for measuring the magnetic moment was the same as that employed in several Λ^0 magnetic-moment measurements.¹⁻⁵ The precession of polarized sigmas in a magnetic field

was measured by observing the asymmetric decay,

$$\Sigma^+ \rightarrow \pi^0 + p. \quad (1)$$

In this experiment the polarization vector was nearly perpendicular to the magnetic field (\vec{B}), while the Σ^+ momentum (\vec{P}_Σ) was directed along \vec{B} . For this case, a Σ that moves a distance L_Σ in the field will have its magnetic moment precess through an angle

$$\epsilon = \mu_\Sigma \Gamma; \quad \Gamma = 2\bar{B}L_\Sigma m_\Sigma / \hbar P_\Sigma, \quad (2)$$

where \bar{B} is the average value of the field along L_Σ , μ_Σ is the magnetic moment in units of

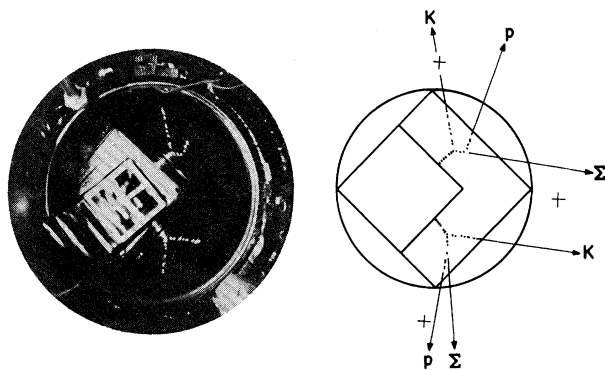


FIG. 1. Picture of sigma event in spark chamber. The spark chamber is located in the bore of the magnet and the two orthogonal views are seen by internal reflection from the spark-chamber frames. The drawing to the right gives the interpretation.

the Bohr nuclear magneton ($\mu_N = e\hbar/2m_p = 3.15 \times 10^{-18}$ MeV/G), and m_Σ is the Σ^+ mass. For this experiment, $(L_\Sigma m_\Sigma / P_\Sigma)_{av}$ was $\sim 1.7\tau_\Sigma$ and $\bar{B} \sim 10^5$ G, giving an average precession angle of 7° per nuclear magneton.

The experimental arrangement⁶ is shown in Fig. 2. Polarized Σ^+ were produced in the reaction



Separated pions ($P_\pi = 1.14$ BeV/c),⁷ obtained from an internal Bevatron target, were directed onto $12 \frac{1}{8}$ -in. polyethylene targets (a total

of 3.59 g/cm²), which formed alternate plates of the first three inches of a spark chamber. The last inch and three-quarters contained $14 \frac{1}{8}$ -in. gaps and was free of target material (see inset of Fig. 2). This chamber was placed directly in the bore of a pulsed solenoidal magnet. The K^+ from Reaction (3) passed through the magnet and into a K detector which was used to trigger the spark chamber. The production and decay Reactions (3) and (1) were visible in the spark chamber (Fig. 1). The spark-chamber frames were designed so that light from the active volume was internally reflected by the frames out of the magnet bore. No adverse effects were observed from the operation of the chamber in the intense magnetic field; on the contrary, a considerable brightening of the sparks was observed which increased the efficiency for detecting valid events. (See later paragraphs concerning the analysis.) The K detector, shown schematically in Fig. 2, consisted of an array of scintillation counters, Cherenkov counters, and absorbers which first selected the production angle, velocity, and range of the K^+ , and then detected its decay. The detector was divided into four quadrants which covered 360° of azimuth from the target, and accepted kaon laboratory production angles between 6 and 30° . The prompt- K^+ signature, $S_\pi S_1 S_2 \bar{C}_2 \bar{C}_5 \bar{C}_3 \bar{C}_4 \bar{S}_3$, opened a 5- to 36-nsec gate. The spark chamber was

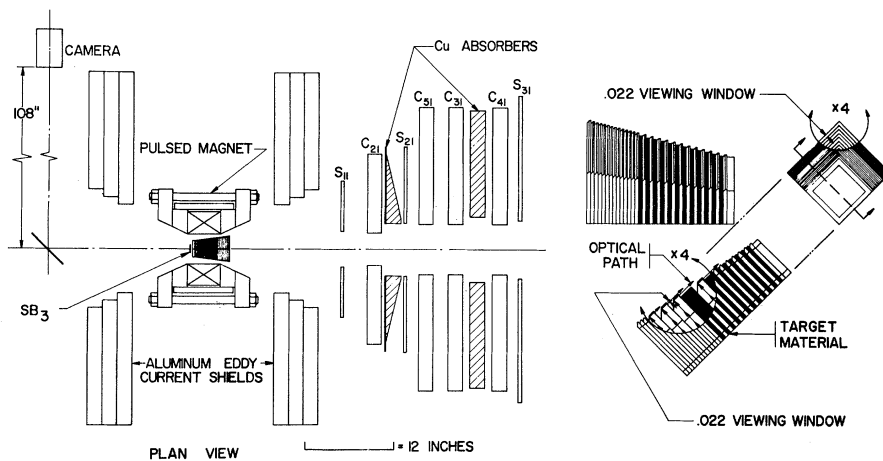


FIG. 2. Experimental arrangement, showing the relative position of the spark chamber, magnet, camera and optics, and the K detector described in text for a single quadrant. The eddy-current shields reduced the field in the region of the detector to tolerable levels. The spark-chamber drawing at right shows the construction of the chamber and the manner in which the light was brought out from the active volume. SB_3 is a scintillation counter defining the beam into the spark chamber, and is part of the incident pion signature defined as S_π . The spark chamber is triggered by $S_\pi S_1 S_2 \bar{C}_2 \bar{C}_5 \bar{C}_3 \bar{C}_4 \bar{S}_3$ which opens a 5- to 36-nsec gate within which a kaon decay signature $C_5 C_3 \bar{C}_4 \bar{S}_3$ or $C_4 S_3 \bar{C}_5 \bar{C}_3$ is required.

triggered by the kaon decay signature, $C_5 C_3 \bar{C}_4 \bar{S}_3$ or $C_4 S_3 \bar{C}_5 \bar{C}_3$, in time coincidence with the gate. S_π was a beam signature which identified the incident pion. The magnet system was an enlarged version of those previously used at the University of Washington.⁸ The magnet produced a peak field of 165 kG at the center of a cylindrical volume 4 in. in diameter and $4\frac{3}{4}$ in. long.

Data were taken with the magnetic field parallel ("normal") or antiparallel ("reversed") to the incident beam direction, and with field off. A total of 1.26×10^{10} pions traversed the target, resulting in about 3×10^5 pictures. The pictures were quick scanned for possible Σ^+ candidates⁹ from which 3000 events were selected for measurement. A measured event was accepted as a valid Σ^+ if (a) the production coplanarity, $\Lambda \equiv \cos^{-1}[(\hat{\pi} \times \hat{\Sigma}) \cdot (\hat{\pi} \times \hat{K})]$, was less than 20° ; (b) the measured sigma production angle, $\theta_{\Sigma \text{ meas}}$, and the sigma production angle calculated from the measured kaon production angle, $\theta_{\Sigma \text{ calc}}$, differed by less than 6° , $\Delta \equiv |\theta_{\Sigma \text{ meas}} - \theta_{\Sigma \text{ calc}}| < 6^\circ$; (c) the measured angle $\theta_{\hat{p}\Sigma}$ between \hat{p} and $\hat{\Sigma}$ was less than the maximum possible for the proton decay mode. (This eliminates all but 5% of the charged-pion decay mode). In addition, Σ -track-length and fiducial-volume restrictions were imposed. Distributions of Λ , Δ , and $\theta_{\hat{p}\Sigma}$ showed peaks of at least 10:1 above background and the widths of Λ and Δ were commensurate with the measured resolutions. The measured resolution on the projected angles was $\pm 5^\circ$ for $\hat{\Sigma}$, and $\pm 30^\circ$ for \hat{K} and \hat{p} . This results in measurement errors on Λ , Δ , and $\theta_{\hat{p}\Sigma}$ of 5, 5, and $\pm 10^\circ$, respectively. The measured lifetime of our accepted sample was $(0.80 \pm 0.07) \times 10^{-10}$ sec, in good agreement with the accepted value. There are essentially no events beyond three lifetimes, and the lifetime plot follows an exponential quite well. Background events in the spark chamber can arise from production processes in which one of the reaction products rescatters. We have estimated this for elastic π - p scattering and various inelastic pion processes (including Fermi momentum). We find that the restriction imposed by (b) and (c) limit the number of such background events in our final sample to less than 10%. On the basis of all of the above evidence, we are confident that we are indeed observing "elastic" Σ^+ production and its subsequent decay into the proton mode. The total number of survived

Table I. Results of the maximum likelihood analysis for two sets of selection criteria. The data used in the "tight" selection analysis are a subset of those used in the "loose" analysis (see text).

	No. of events	$\alpha \bar{P}$	μ_{Σ}^*
"Tight" selection criteria			
Field normal	92	} -0.86 ± 0.09	1.3 ± 1.3
Field zero	146		
Field reversed	143	} -0.64 ± 0.10	1.8 ± 1.5
All data	381		
"Loose" selection criteria			
Field normal	123	} -0.86 ± 0.09	2.2 ± 1.3
Field zero	186		
Field reversed	177	} -0.56 ± 0.09	1.0 ± 2.0
All data	486		

Σ^+ events is given in Table I.

The expected distribution of the decay proton in the angle χ defined in Fig. 3 is

$$dn(\chi) = (N/2\pi)[1 + K \cos(\chi + \Gamma\mu_{\Sigma})]d\chi, \quad (4)$$

where $K = \pi\alpha\bar{P}/4$, \bar{P} is the average polarization of the Σ , α is the decay asymmetry param-

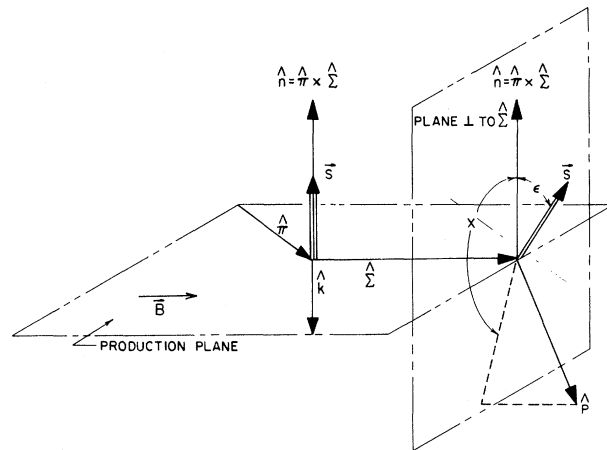


FIG. 3. Description of the vectors pertinent to the production and decay Reactions (5) and (1) in the text. The vectors \hat{K} , $\hat{\pi}$, $\hat{\Sigma}$, \hat{p} are unit vectors in direction of the kaon, pion, sigma, and proton momenta, respectively; \vec{S} is the spin vector of the sigma, and \vec{B} is the magnetic-field vector in the "normal" position.

ter, and μ_Σ is defined in Eq. (2). N is the total number of decay events. In this experiment Γ and χ are measured for each event, hence a two-parameter likelihood analysis would experimentally determine both K and μ_Σ . However, the χ distribution of our "field-off" data is noticeably different from the distribution (4) with $\Gamma = 0$. It is evident from Fig. 4(a) that there is a pronounced deficiency in the region $140 \leq \chi \leq 230^\circ$. This indicates an experimental bias. The effect also persists in the "field-on" data. Previous hyperon magnetic moment analyses^{4,5} have also had to contend with similar biases, and the approach has been simply to delete the biased portion of the data. This method does not introduce a serious systematic error if the bias is small; however, for larger biases, the "cutoff" is most certainly arbitrary and we therefore made an independent experimental determination of the bias. Tests made on the χ distributions, in which the spark-chamber fiducial volume was restricted to regions of varying distance from the spark-chamber walls, indicated clearly that the bias was predominantly due to fiducial volume. On the basis of this evidence, events were created using a Monte Carlo technique to determine the effect on the χ distribution introduced by the small spark-chamber fiducial volume. First, measurements were made on all the accepted events to determine the number of Σ^+ sparks, the number of proton sparks, and the number of K sparks needed to allow identification of an event. In addition, measurements were made to determine the spark formation efficiency for each of these particles. The "created" events were then tested using the measured sparking efficiency and spark-number criteria to determine if they could be identified before leaving the chamber. The χ distribution of the surviving events from this Monte Carlo analysis was fitted by a four-term Fourier expansion. Separate functions were generated for "field-on" [$E_f(\chi)$] and "field off" [$E_o(\chi)$] since the spark brightness and, therefore, the spark detection efficiency were not the same for the two cases. In Fig. 4(a) we show a comparison of $E_o(\chi)(1 + K \cos \chi)$ with the experimental χ distribution of our accepted events for the "field-off" case. A similar plot for the "field-on" data is shown in Fig. 4(b). We have included events for both signs of field to improve the statistics for comparison with the theoretical distribution. To make such a comparison possible it is neces-

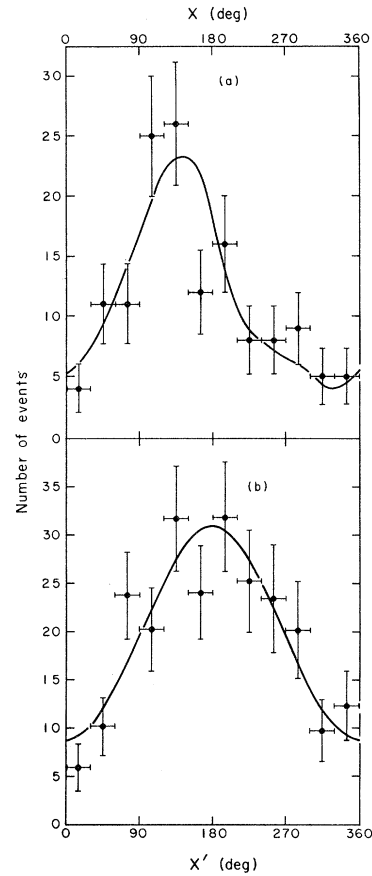


FIG. 4. (a) "Field-off" data. The curve is the function $(1 + K \cos \chi)E_o(\chi)$, normalized to 140 events, with $K = -0.56$, the value found in this experiment. (b) "Field-on" data. The histogram and the smooth curve are described in the text. The degree of agreement between the histogram and the smooth curve is a measure of the validity of our bias calculation.

sary to "unwind" each event. This we do by forming the quantity $\chi_i' = \chi_i + \Gamma_i \mu_\Sigma$ for all "field-on" events, where χ_i is the measured angle for the i th event and μ_Σ is our experimental value for the magnetic moment. These events weighted by $[E_f(\chi_i' - \Gamma_i \mu_\Sigma)]^{-1}$ are used to form the histogram in Fig. 4(b). This histogram is to be compared with the smooth curve

$$N(\chi')d\chi' = (N_f/2\pi)(1 + K \cos \chi')d\chi'.$$

With the inclusion of the bias, the likelihood function becomes

$$\mathcal{L}(\mu_\Sigma, K) = \prod_{i=1}^N E_f(0)(\chi_i) \times [1 + K \cos(\chi_i + \Gamma_i \mu_\Sigma)] A_i^{-1}, \quad (5)$$

$$A_i = \int_0^{2\pi} E_f(0)(\chi) [1 + K \cos(\chi_i + \Gamma_i \mu_\Sigma^*)] d\chi. \quad (6)$$

A two-parameter maximum-likelihood calculation was made to determine the best values for the magnetic moment (μ_Σ^*) and the asymmetry parameter (K^*). Table I gives the results of these calculations. Entries are made for the two field directions analyzed separately, and for two different sets of data-selection criteria. The "tight" criteria refer to the selection described above, while the "loose" applies to somewhat relaxed kinematic and fiducial-volume requirements. For the correct bias function, the results from the two field directions should agree. For the "tight" selection criteria good agreement is obtained. The somewhat greater disagreement between the results for the two field directions for the "loose" data, while not statistically unlikely, is attributable, in part, to differences in the requirements for detection of events in the two sets. The same bias function was used in both analyses. We expect that the agreement could be improved by determining the correct bias function for the "loose" data in the same way that it was determined for the "tight" data. The result obtained by combining the data from both field directions should be quite insensitive to this type of bias. We have varied the bias function over wide limits and have found that the values obtained for μ_Σ^* and K^* stay well within our quoted errors. For example, if the bias function is set equal to unity (i.e., the bias is ignored), the value of μ_Σ^* obtained is 1.3, still well within our error. However, the value obtained for the separate field directions (when the bias is ignored) is 0.0 and 4.0 for normal and reversed, respectively.¹⁰ For the two different selection criteria, the results for μ_Σ^* and K^* for the combined data (two field directions) are within the quoted error, showing the relative insensitivity of our result to the selection criteria.

The sign of our result is positive and our convention is the following: A positive magnetic moment will precess counterclockwise looking along the direction of the magnetic field (see Fig. 3). The direction of the magnetic field was determined during the experiment by checking the polarities of the magnet and magnet power supply, and was confirmed during the analysis by observation of track curva-

ture for particles in easily recognized events (e.g., Λ^0 's and the longest lived Σ 's).

Estimates have shown that systematic errors in K^* and μ_Σ^* are negligible when compared to the statistical errors. The errors (standard deviation) quoted in Table I are purely statistical, and were calculated using standard error analysis methods.¹¹

The symmetry schemes SU(3) and SU(6),^{12,13} in the absence of the mass-splitting interactions, both predict that $\mu_\Sigma = \mu_b = 2.79$. The mass-corrected value of Bég and Pais¹⁴ is $\mu_\Sigma = 2.2$. The errors associated with these predictions, as well as other model-dependent calculations,¹⁵ may well be the order of this difference or larger. The value $\mu_\Sigma = 1.5 \pm 1.1$, obtained in this experiment, is in agreement with these predictions within the limited accuracy, and the experiment indicates that there are no large anomalies.¹⁶

We wish to thank Professor R. W. Williams for his many contributions to this experiment. We would also like to acknowledge the contributions of Dr. Y. B. Kim who first initiated the pulsed high magnetic field work at the University of Washington, and who pointed out the applicability of this facility to the measurement of magnetic moments. J. Humphrey, O. Sander, and D. Nygren contributed to the design and running of the experiment. We wish to thank D. E. J. Lofgren and the Bevatron staff for their cooperation. The technical assistance of J. Schultz, A. Olsen, M. Rongerude, and F. Toevs is greatly appreciated.

*Research supported in part by the University of Washington and by the National Science Foundation.

†Present address: Applied Physics Laboratory, University of Washington, Seattle, Washington.

‡Present address: Physics Department, University of California, San Diego, La Jolla, California.

§Present address: Physics Department, University of Illinois, Urbana, Illinois.

|| Present address: Physics Department, Brookhaven National Laboratory, Upton, New York.

¹R. L. Cool, E. W. Jenkins, T. F. Kycia, D. A. Hill, L. Marshall, and R. A. Schluter, *Phys. Rev.* **127**, 2223 (1962).

²W. Kernan, T. B. Novey, S. D. Warshaw, and A. Wattenberg, *Phys. Rev.* **129**, 870 (1963).

³J. A. Anderson and F. S. Crawford, Jr., *Phys. Rev. Letters* **13**, 167 (1964).

⁴G. Charrier, M. Gailloud, P. Rosset, R. Weill, W. M. Gibson, K. Green, P. Tolun, N. A. Whyte, J. C. Combe, E. Dahl-Jensen, N. T. Doble, D. Evans, L. Hoffman, W. T. Toner, H. Going, K. Gottstein, W. Puschel, V. Scheuning, and J. Tietge, *Phys. Lett.*

ters 15, 66 (1965).

⁵D. Hill, K. Li, E. Jenkins, T. Kycia, and H. Ruder-
man, Phys. Rev. Letters 15, 85 (1965).

⁶A complete description of the experimental appara-
tus will be published elsewhere.

⁷During the experiment, measurements of the Σ^+
polarization were also made at a pion momentum of
1.18 BeV/c. Over the acceptance region of our detec-
tor ($\cos\theta_{\Sigma^*} = -0.16$ to -0.93), we obtain the result
 $\alpha P = -0.20 \pm 0.15$. Because of this indication of a pos-
sible low αP , we reduced our pion momentum to 1.14,
where there was stronger evidence of a large polariza-
tion from other sources.

⁸Y. B. Kim and E. Platner, in Proceedings of the
International Conference on High Magnetic Fields,
Cambridge, Massachusetts, 1961, edited by H. Kolm
et al. (Massachusetts Institute of Technology Press,
Cambridge, Massachusetts, and John Wiley & Sons,
Inc., New York, 1962); E. Platner, J. Orr, G. Masek,
and R. Williams, Nucl. Instr. Methods 20, 505 (1963).

⁹Lambdas from the reaction $\pi^+ + n \rightarrow \Lambda^0 + K^+$ were
also produced and observed. It proved impossible,

however, to separate these from Λ^0 from Σ^0 decays,
and hence, a Λ^0 magnetic moment measurement was
not possible.

¹⁰The value of field reversal in experiments of this
type is clearly illustrated by these results. Not only
does the field aid in the verification of the correct bias
function, but allows the final result (combining the
data of both field directions) to be relatively insensi-
tive to such biases.

¹¹See, e.g., J. Orear, University of California Radia-
tion Laboratory Report No. UCRL-8417 (unpublished).

¹²S. Coleman and S. L. Glashow, Phys. Rev. Letters
6, 423 (1961).

¹³M. A. B. Béq, B. W. Lee, and A. Pais, Phys. Rev.
Letters 13, 514 (1964).

¹⁴M. A. B. Béq and A. Pais, Phys. Rev. 137, B1514
(1965).

¹⁵For example, H. Pagels, Phys. Rev. 140, B999
(1965).

¹⁶A previous emulsion experiment [A. D. McInturff
and C. E. Roos, Phys. Rev. Letters 13, 246 (1964)]
found $\mu_{\Sigma} = 4.3 \pm 1.5$.

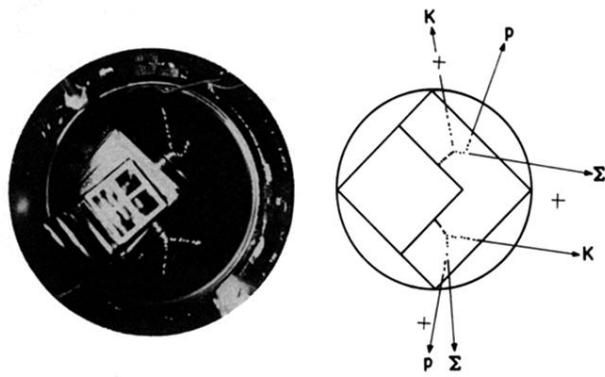


FIG. 1. Picture of sigma event in spark chamber. The spark chamber is located in the bore of the magnet and the two orthogonal views are seen by internal reflection from the spark-chamber frames. The drawing to the right gives the interpretation.